International Conference on Applied Energy 2019
Aug 12-15, 2019, Västerås, Sweden
Paper ID: # 506

SIMULATION ON MICRO-CHANNEL VERTICAL EVAPORATOR FOR RACK-BACKDOOR COOLING OF DATA CENTER UNDER VARIABLE HEAT LOAD

Binfei Zhan[1,2,3], Shuangquan Shao[1,2], Mingsheng Tang[1,2], Hainan Zhang[1,2], Changqing Tian[1,2,3], Yuan Zhou[1,2]

1 Key Laboratory of Cryogenics, Technical Institute of Physics and Chemistry, Chinese Academy of Sciences, Beijing 100190, China

2 Beijing Key Laboratory of Thermal Science and Technology, Technical Institute of Physics and Chemistry, Chinese Academy of Sciences, Beijing 100190, China

3 University of Chinese Academy of Sciences, Beijing 100049, China

ABSTRACT

The rack backdoor cooling is an efficient way for server temperature contral and energy saving. In this paper, a coupled model of multiple-heat-sources model of 42U rack and mathematical models of the micro-channel vertical evaporator are established and mathematical models are verified by experimental results. Inhomogeneous air temperature and flow velocity data after being heated by servers and before coming in evaporator can be obtained with the rack model. It is discovered that the maximum temperature difference is up to 9.5℃ under uniform load conditions, and 15℃ under non-uniform load conditions. When upper, middle and lower parts of the rack are set to zero load, the overall air-side outlet temperature difference can reach 6.5℃, 8℃ and 8.5℃ separately. Compared with full load working, the air temperature uniformity of evaporator outlet can be improved when some severs are standby, and it improves with the height of inactive servers. These simulation results can provide an effective guidance for the optimization design and application of the micro-channel vertical evaporator in the rack backdoor cooling.

Keywords: data center, backdoor cooling, microchannel, vertical tube evaporator, non-uniform load conditions

NONMENCLATURE

Abbreviations

P	pressure, Pa
P_a	accelerational pressure drop, Pa
P_f	frictional pressure drop, Pa
P_g	gravitational pressure drop, Pa
P_l	local pressure drop, Pa
Q	heat transfer rate, W
T	temperature, °C
T_s	wet bulb temperature, °C
V	flow speed, ms^{-1}
G	mass flux, $kgm^{-2}s^{-1}$
h	enthalpy, $kJkg^{-1}$
M	refrigerant charge, kg
σ	difference
α	thermal transfer coefficient, $Wm^{-2}\cdot K^{-1}$
d_e	equivalent diameter, m
L	length, m
λ	thermal conductivity, $Wm^{-1}K^{-1}$
R_e	Reynolds number
B_o	Boiling number
F_r	Froude number

Symbols

con	condenser
eva	evaporator
s	assume
m	momentum
f	frictional
L	liquid
G	gas
f	fluid
t	total
h	refrigerant
a	air
in	inlet
ac	actual
out	outlet
ave	average
up	gas tube
down	liquid tube
chong	refrigerant charge

1. INTRODUCTION

With the development of information technology, the increase of data centers number, energy consumption and heat dissipation density are getting more and more attentions from all of the countries in the world[1-2]. Energy consumption of data center traditional cooling is around 30%-40% of data center total energy consumption[3-4]. Hence some researchers have put forward many efficient technical solutions, as one of them, rack-level cooling can effectively reduce local spots and mixing of cold and hot air due to closer to the heat source. In addition, free cooling has a great advantage by reducing the cost of cold source, such as heat pipe technology. Furthermore, some researchers found that utilizing micro-channel evaporator can improve the performance of the loop thermosyphon system in data center cooling applications[5]. So backdoor cooling technology based on thermosyphon and micro-channel evaporator has great application prospect in data center cooling, which can combine rack level cooling with free cooling. The heat load of the racks in the data center are variable when they are running, hence investigation on backdoor cooling technology based on thermosyphon and micro-channel evaporator under variable heat load is significant for the optimization of system control.

In this paper, a rack physical model is built to obtain simulation parameters of the air inlet of the backdoor evaporator. Micro-channel vertical evaporator model and its applicable thermosyphon loop system calculation model are set up for investigating the performance of the evaporator. This paper provides novel results on the local superheat and inhomogeneous liquid distribution of the evaporator under variable heat load conditions, which can guide further avoidance of these problems.

2. SIMULATION MODEL

2.1 Physical parameters and flow field modeling

The micro-channel vertical tube evaporator consists of header tube, flat tube and louver fin. The micro-channel flat tube size is 1.4mm× 0.9mm, the number of flat tubes is 30, and its length is 1.57 m, the other structural size parameters are shown in Fig. 1. R22 is used as the working fluid.

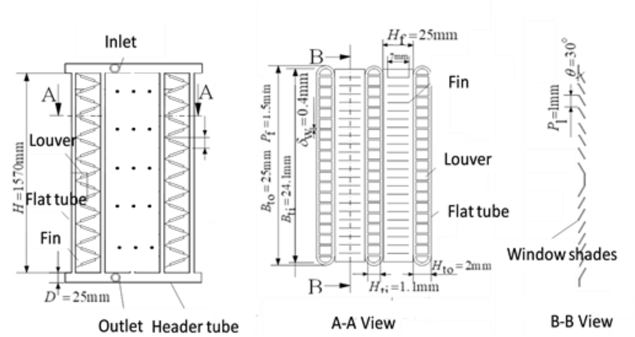

Fig 1 Structure and size of a microchannel flat tube heat exchanger

Main heating components in the server are CPU, computer memories, circuit board. A 2U server model is built based on one practical product, whose size is widely used in center data rack, and its main heating components layout inside is also shown in Fig. 2.

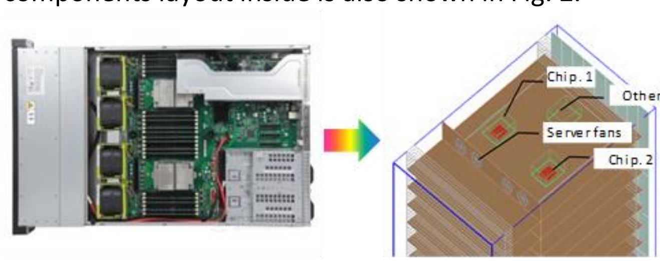

Fig 2 Construction of server structure model

The heating power value of each chip is 80 W, and the rest components including computer memories, circuit board are totally 126 W, so the total heating power value of each server is 286 W and of the whole rack is 6 kW.

A 42U standard rack model of 0.6 m wide, 2 m high and 1 m deep is built with ICEPAK software. The model rack is arranged 21 layers of 2U servers for making full use of space. The hole plate whose opening rate is 0.5 is set separately before and after the rack, fans numbers configured in the rack backdoor is 10, as shown in Fig. 3.

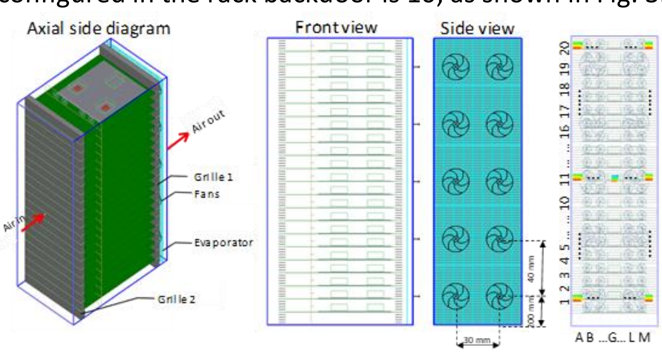

Fig 3 The model structure of the cabinet and the layout of the fans and severs

In order to improve the calculation accuracy and sectional research, the evaporator is divided into 20 rows (number 1-20) in the vertical direction and 13 columns (number A-M) in the horizontal direction, total 260 microelements. The rack model is symmetrical in the horizontal direction due to the layout of severs and fans.

2.2 Evaporator modeling

Air-side thermal transfer coefficient of the evaporator is calculated as Gogol correlation：

$$\partial_{\mathrm{a}} = c_1 c_2 \left(\frac{\lambda}{d_{\mathrm{e}}}\right)\left(\frac{L}{d_{\mathrm{e}}}\right)^{\mathrm{n}} R_{\mathrm{e}}^{\mathrm{m}} \qquad (1)$$

Refrigerant-side two-phase heat transfer coefficient of the evaporator is calculated as Kandlikar correlation:

$$\frac{h_{\mathrm{tp}}}{h_L} = C_1 C_0^{C_2}\left(25 Fr_{L_O}\right)^{C_5} + C_3 B_0^{C_4} F_{\mathrm{f}L} \qquad (2)$$

Refrigerant-side single-phase heat transfer coefficient of the evaporator is calculated as Dittus-Boelter correlation:

$$Nu_{\mathrm{f}} = 0.023 Re_{\mathrm{f}}^{0.8} Pr_{\mathrm{f}}^{n} \qquad (3)$$

The total pressure drop, $\triangle p_{\mathrm{t}}$, in the tube corresponds to the sum of four parts, including the gravity pressure drop, $\triangle p_{\mathrm{g}}$, momentum pressure drop, $\triangle$pm, frictional pressure drop, $\triangle$pf, and local pressure drop, $\triangle p_{\mathrm{l}}$:

$$\Delta p_t = \Delta p_g + \Delta p_{\mathrm{a}} + \Delta p_f + \Delta p_l \qquad (4)$$

In the refrigerant-side single phase pressure drop model, the tube section is a vertical and constant pipe diameter. That is, accelerational pressure drop, $\triangle p_{\mathrm{a}}$, and local pressure drop, $\triangle p_{\mathrm{l}}$, are all equal to zero, as Blasius correlation:

$$-\frac{dp}{dz} = \rho g \sin\theta + \lambda \frac{dz}{d}\frac{G^2}{2\rho} \qquad (5)$$

In the refrigerant-side two phase pressure drop model, frictional pressure drop $\triangle p_{\mathrm{l}}$ is calculated as:

$$-\frac{dp}{dz} = \left(\alpha\rho_G + (1-\alpha)\rho_L\right) g dz \sin\theta + G^2 d\left(\frac{(1-x)^2}{\rho_L(1-\alpha)} + \frac{x^2}{\rho_G \alpha}\right) + dp_{\mathrm{f}} \qquad (6)$$

$\triangle$ pf is calculated as Lockhart and Martinelli correlation:

$$\left(\frac{dp}{dz}\right)_{\mathrm{f}} = \left(\frac{dp}{dz}\right)_L \phi_L^2 \quad , \quad \phi_L^2 = 1 + \frac{C}{X_{tt}} + \frac{1}{X_{tt}^2} \qquad (7)$$

$$\left(\mathrm{Re}_L > 4000\right)$$

$$\left(\frac{dp}{dz}\right)_{\mathrm{f}} = \left(\frac{dp}{dz}\right)_G \phi_G^2 \quad ,$$

$$\phi_G^2 = 1 + C X_{tt} + X_{tt}^2 \left(\mathrm{Re}_L < 4000\right) \qquad (8)$$

$$\left(\frac{dp}{dz}\right)_L = f_L \frac{2G^2}{D\rho_L}(1-x)^2 \quad ,$$

$$\left(\frac{dp}{dz}\right)_G = f_g \frac{2G^2}{D\rho_G} x^2 \qquad (9)$$

$$f_i = \frac{16}{\mathrm{Re}_i} \quad \left(\mathrm{Re}_i < 2000\right) \quad , \quad f_i = \frac{0.079}{\mathrm{Re}_i^{0.25}} \quad \left(\mathrm{Re}_i > 2000\right) \qquad (10)$$

$$Re_L = \frac{GD}{\mu_L}(1-x) \quad , \quad Re_G = \frac{GD}{\mu_G} x \qquad (11)$$

$$X_{tt} = \left(\frac{1-x}{x}\right)^{0.9}\left(\frac{\rho_G}{\rho_L}\right)^{0.5}\left(\frac{\mu_L}{\mu_G}\right)^{0.1} \qquad (12)$$

C-value, λ_l, λ_g-value are chose as table 1.

Table 1. *C*-value, λ_l, λ_g-value under different flow states

Liquid	Gas	C-value	λ_l, λ_g-value
Laminar	Laminar	5	$\lambda_l = \frac{64}{\mathrm{Re}_l}, \lambda_g = \frac{64}{\mathrm{Re}_g}$
Laminar	Turbulent	12	$\lambda_l = \frac{64}{\mathrm{Re}_l}, \lambda_g = \frac{0.184}{\mathrm{Re}_g^{0.2}}$,
Turbulent	Laminar	10	$\lambda_l = \frac{0.184}{\mathrm{Re}_l^{0.2}}, \lambda_g = \frac{64}{\mathrm{Re}_g}$
Turbulent	Turbulent	20	$\lambda_l = \frac{0.184}{\mathrm{Re}_l^{0.2}}, \lambda_g = \frac{0.184}{\mathrm{Re}_g^{0.2}}$

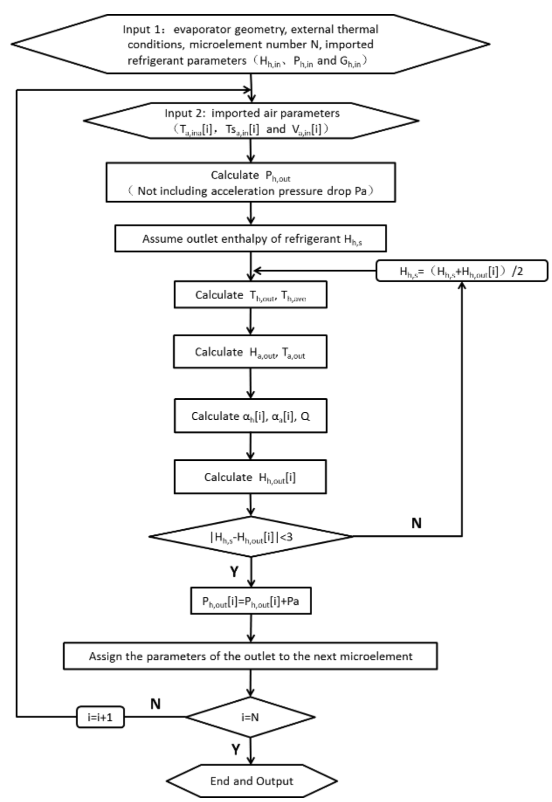

Fig 4 Flow chart of iterative calculation for vertical tube evaporator

Using VC-6.0 software, the model calculation process is designed as shown in Fig. 4, in which the vertical tube heat exchanger is divided into 20 microelements in the vertical direction. The export parameters of each micro element are assigned to the exit parameters of the next microelement, and the distribution parameter method is used to iteratively calculate the parameters of the refrigerant.

2.3 Model verification

In order to verify the evaporator model, the heat pipe loop model including micro-channel vertical evaporator, condenser, gas tube and liquid tube is further established to compare with the experimental data. The simulation calculation program of the loop thermosyphon system is shown in Fig. 5. First, the inlet pressure, the inlet enthalpy value and the circulation mass flow of the evaporator are assumed respectively. Then, the evaporator, the gas tube, the condenser and the liquid tube are calculated according to the program. The inlet pressure and the enthalpy value of the evaporator are finally obtained by the iterative calculation.

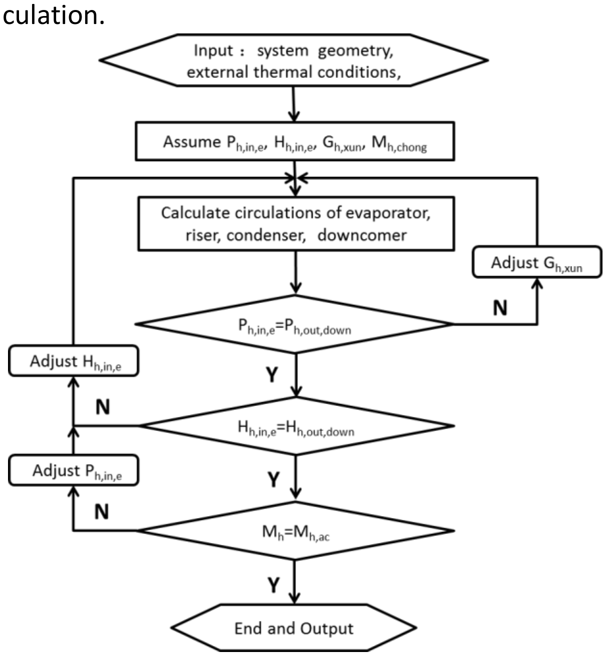

Fig 5 Flow chart of simulation calculation for loop thermosyphon system

The height difference between the outlet of the condenser and the evaporator is set as 2.2m. The pipe diameter of the riser is 19mm, and the length is 2.56m. The pipe diameter of the down comer is 16mm, and the length position is 4.65m. In the experimental test, the indoor temperature is 35℃, the wet bulb temperature is 23.9℃, and the inlet air volume of the backdoor evaporator is 1800 m^3/h.

The experimental data of the outlet air tempereature and the outlet refrigerant are obtained from Xiao et al.[6], which are compared with the results of the model calculation. The specific comparison results are shown in Fig. 6.

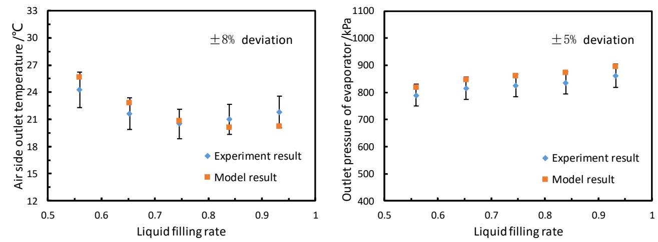

Fig. 6. Comparison between experimental results and model calculation results of air outlet temperature and outlet pressure evaporator

As shown in the Fig.6, the outlet air temperature deviation and the outlet refrigerant pressure deviation between the simulation results and the experiment results are within ±8% and ±5% respectively. It indicates that the simulation model has high accuracy.

3. PERFORMANCE ANALYSIS

The inlet temperature is initially set at 15℃. The refrigerant state of inlet is set as saturated liquid phase for ensuring that the refrigerant can evaporate within transition phase to the greatest extent. The temperature of the indoor dry-ball was 30℃ and the wet-bulb temperature was 18℃ for ensuring that the evaporator surface can not produce dews. The evaporator is divided into 20 microelements in the vertical direction.

As the height of the backdoor evaporator is obviously higher than the height of the general evaporator, the local variation of air inlet wind speed and temperature will affect the heat transfer performance of the whole evaporator, so the airside inlet conditions of the evaporator cannot be set as uniform.

3.1 Simulations under Invariable load conditions

Due to the different thermal load and position of the rack server, the air side inlet temperature is different; Due to the different position and structure of backdoor fan and other wind resistances, the air side inlet wind speed is different, as shown in Fig. 7. Therefore, setting the air side inlet conditions of the evaporator based on the actual conditions can improve the accuracy of model calculation and help study the local heat transfer process of evaporator.

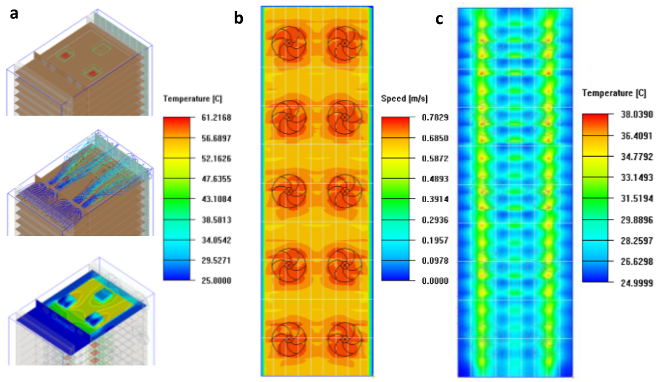

Fig 7 Air side inlet inhomogeneous temperature and wind speed of evaporator under variable heat load conditions

3.2 Simulations under variable load conditions

Above is the simulation results of the rack's servers running at full load, but in some cases, the rack 's servers are out of standby state, and there is almost no hot load. So the upper (b), middle (c) and lower (d) parts of the rack are set to zero load, as shown in the following figure.

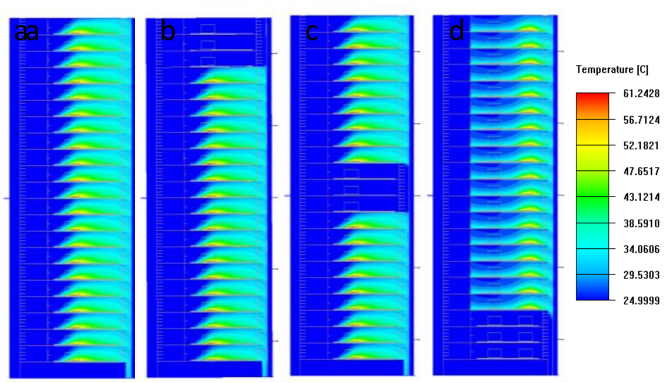

Fig 8 Upper (b), middle (c) and lower (d) parts of the rack are set to zero load

From the Fig. 9, it can be seen that the maximum air-side temperature difference of evaporator outlet is about 9.5℃, due to the overheating of refrigerant in the tube outlet of evaporator, and the overall air-side outlet temperature difference can reach 6℃ under full heat load condition, even if disregarding the effect of overheating. And when upper, middle and lower parts of the rack are set to zero load, the overall air-side outlet temperature difference can reach 6.5℃, 8℃ and 8.5℃ separately.

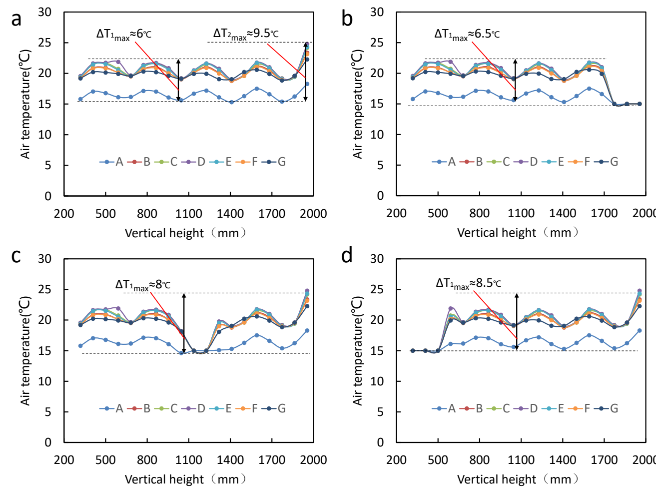

Fig 9 The air side outlet temperature of the evaporator vary with the position of the vertical microelement (a. full load, b. Upper, c. middle, d. lower are set as zero load)

4. CONCLUSIONS

The maximum air-side temperature difference of evaporator outlet is about 9.5℃, due to the overheating of refrigerant in the tube outlet of evaporator, and the overall air-side outlet temperature difference can reach 6℃ under full heat load condition, even if disregarding the effect of overheating. And when upper, middle and lower parts of the rack are set to zero load, the overall air-side outlet temperature difference can reach 6.5℃, 8℃ and 8.5℃.

From the calculation results, it can be concluded that when some servers are not working, compared with full load working, the uniformity of evaporator outlet air temperature can be improved, and the outlet temperature uniformity improves with the height of inactive servers. Further, air temperature uniformity needs to be compared when some servers are down under the same load.

ACKNOWLEDGEMENT

The authors gratefully acknowledge the financial supports from National Key R&D Program of China (2017YFE0105800) and National Natural Science Foundation of China (No. 51676199 and No. 51706232).

REFERENCE

[1] Cho. K, Chang. H, Jung. Y, Yoon. Y, Economic analysis of data center cooling strategies. Sustainable Cities and Society, 2017, 31:234-243. (Reference to a journal publication)

[2] Nadjahi. C, Louahlia. H, Lemasson. S, A review of thermal management and innovative cooling strategies for data center. Sustainable Computing Informatics & Systems, 2018, 19:14-28. (Reference to a journal publication)
[3] Zakarya M. Energy, performance and cost efficient datacenters: A survey. Renewable & Sustainable Energy Reviews, 2018, 94:363-385. (Reference to a journal publication)
[4] Dayarathna M, Wen Y, Fan R. Data Center Energy Consumption Modeling: A Survey. IEEE Communications Surveys & Tutorials, 2017, 18:732-794. (Reference to a journal publication)
[5] Yue. C, Zhang Q, Zhai Z, Ling L, Numerical investigation on thermal characteristics and flow distribution of a parallel micro-channel separate heat pipe in data center, International Journal of Refrigeration, 2019, 98:150-160. (Reference to a journal publication)
[6] Xiao X, Zhang Q, Ling L, Yue C, Lou Jn , Yi J, Experimental study on the optimal refrigerant filling ratio of micro-channel rear door type heat pipe system, Journal of Refrigeration, 2018.45-50. (Reference to a journal publication)